

Studies of Diffusional Mixing in Rotating Drums via Computer Simulations

G.A. Kohring

Central Institute for Applied Mathematics

Research Center Jülich (KFA)

D-52425 Jülich, Germany

g.kohring@kfa-juelich.de

Abstract

Particle diffusion in rotating drums is studied via computer simulations using a full 3-D model which does not involve any arbitrary input parameters. The diffusion coefficient for single-component systems agree qualitatively with previous experimental results. On the other hand, the diffusion coefficient for two-component systems is shown to be a highly nonlinear function of the rotation velocity. It is suggested that this results from a competition between the diffusive motion parallel to, and flowing motion perpendicular to the axis of rotation.

(submitted to *Journal de Physique*)

1 Introduction

Rotating drums perform critical functions in many industrial processes. They are utilized for tasks such as humidification, dehumidification, convective heat transfer, facilitation of gas-solid catalytic reactions and, not the least, ordinary mixing or blending. Understanding the mechanisms behind particle

mobility in rotating drums is an important step towards refining the efficiency of such processes. In the absence of mechanical agitators, momentum is imparted to the particles only in the plane perpendicular to the rotation axis. Motion parallel to the axis of rotation occurs through momentum changes induced by the collisions between particles. Since these collisions occur more or less randomly in time, this motion is diffusive in nature. Until now most computer simulations have neglected the essential three-dimensional character of these systems and, via two-dimensional simulations, concentrated on the motion perpendicular to the rotation axis [1]. In the present work the diffusive motion in the longitudinal direction is examined using a full three-dimensional model.

Previous experimental studies of diffusive motion in rotating cylinders have concentrated on single-component systems, i.e., a cylinder partially filled with a single particle type [2, 3]. One-half of the particles were dyed a different color in order to make them distinguishable. These diffusion experiments were simplified through the use of an ideal starting arrangement: initially, the colored particles are axially segregated so that mixing occurs only through the diffusive motion parallel to the rotation axis. Under these ideal circumstances, some aspects of the diffusive mixing can be studied analytically and Hogg et al. [2] obtained good agreement between the theory and experiment.

The present study focuses on diffusion in two-component systems. Diffusion in two-component systems is expected to exhibit characteristics not found in single-component systems, because the former have been shown to exhibit spontaneous material segregation [4]. In this form of segregation several bands parallel to the rotation axis are formed. These bands alternate between the two material types and there is normally an odd number of such bands. The nature of this phenomena is not completely understood, however, it is clear that diffusion must play an important role. Indeed the results to be presented here demonstrate a distinct difference between the diffusion in 1-component and 2-component systems.

In the following section, a three dimensional model for colliding, visco-elastic spheres is presented and its numerical implementation is discussed. The next section describes the experimental arrangement. Following that, the results are presented and discussed. The paper concludes with some speculative comments on the mechanisms behind material segregation in rotation drums.

2 A Computational Model for Visco-Elastic, Mesoscopic, Spherical Particles

The contact-force model presented here is based upon a visco-elastic model for the collision of two mesoscopic, spherical particles developed over the last 100 years by Hertz [5], Johnson et al. [6], Kuwabara and Kono [7] and Mindlin [8]. This model is free of arbitrary parameters in the sense that all input variables are material properties amenable to experimental verification. The model involves four key elements: 1) particle elasticity, 2) energy loss through internal friction, 3) attraction on the contact surface and 4) energy loss through the action of frictional forces.

2.1 Particle Elasticity

As demonstrated by H. Hertz [5], the deformation of elastic particles of finite extent leads to a nonlinear dependence between the compressive force and the compression length.

$$\mathbf{F}_{ij}^{\text{elastic}} = \frac{4}{3} \frac{E_i E_j}{E_i (1 - \nu_j^2) + E_j (1 - \nu_i^2)} \sqrt{\frac{R_i R_j}{R_i + R_j}} h_{ij}^{3/2} \mathbf{n}_{ij}^{\perp}, \quad (1)$$

where,

$$h_{ij} = R_i + R_j - |\mathbf{X}_i - \mathbf{X}_j|, \quad (2)$$

and,

$$\mathbf{n}_{ij} = \frac{\mathbf{X}_i - \mathbf{X}_j}{|\mathbf{X}_i - \mathbf{X}_j|}. \quad (3)$$

Here, R_i symbolizes the radius of the i -th particle. E_i represents the elastic modulus and ν_i the Poisson ratio. \mathbf{X}_i is the position vector of the i -th particle and \mathbf{n}_{ij}^{\perp} indicates a unit vector pointing from grain j to grain i perpendicular to the contact surface. (Because all the forces described here are contact forces, they are nonzero only if $h_{ij} > 0$.)

2.2 Internal Friction

Energy dissipation due to the viscous nature of the solid particles was first studied by Kuwabara and Kono [7] more than a century after Hertz's work.

They obtained the following expression for the non-conservative viscous force acting during a collision:

$$\mathbf{F}_{ij}^{\text{viscos}} = -2 \frac{B_i B_j}{B_i (1 - \sigma_j^2) + B_j (1 - \sigma_i^2)} \sqrt{\frac{R_i R_j}{R_i + R_j}} h_{ij}^{1/2} \mathbf{v}_{ij}^{\perp}, \quad (4)$$

where,

$$B_i = \frac{9\xi_i\eta_i}{3\xi_i + \eta_i} \quad (5)$$

and,

$$\sigma_i = \frac{3\xi_i - 3\eta_i}{2(3\xi_i + \eta_i)}. \quad (6)$$

ξ_i and η_i are the coefficients of viscosity associated with volume deformation and shear. \mathbf{v}_{ij}^{\perp} is the relative velocity of the colliding particles normal to the contact surface.

2.3 Surface Attraction

When two surfaces are brought into contact an attractive force due to the attractive part of the inter-molecular interaction arises. The case of spherical particles composed of molecules interacting via a Lennard-Jones potential was first studied by Hamaker [9] for non-elastic grains. It was extended to the case of elastic grains by Dahneke [10]. The form used here was introduced by Johnson et al. [6] for a general molecular interaction characterized by the surface energy, W_{ij} , of the contacting materials.

$$\mathbf{F}_{ij}^{\text{meso}} = -\sqrt{\frac{4}{3} \frac{8\pi W_{ij} E_i E_j}{E_i (1 - \nu_j^2) + E_j (1 - \nu_i^2)}} \left(\frac{R_i R_j}{R_i + R_j}\right)^{1/4} h_{ij}^{3/4} \mathbf{n}_{ij}^{\perp} \quad (7)$$

Note the small power, 1/4, to which the reduced radius is raised. Since the weight of a spherical grain is equal to $4/3\pi\rho g R^3$, there will be a grain size for which the weight of a particle is equal in magnitude to this attractive force. Particles smaller than this critical size experience this interaction as an adhesive. Typically, this critical grain size is on the order of 1 mm [11]. For grain sizes much larger than about 1 cm, this force can be neglected.

2.4 External Friction Forces

The frictional forces which develop under conditions of slip parallel to, or rotation about the normal to the contact surface were first studied by Mindlin [8]. Mindlin's original expression is computationally expensive, therefore a simplified expression is used which amounts to assuming that no partial slipping of the contact surfaces occurs.

$$\mathbf{F}_{ij}^{\text{shear}} = \min \left(\frac{16}{3} \frac{G_i G_j \delta s}{G_i (2 - \nu_j) + G_j (2 - \nu_i)} \sqrt{\frac{R_i R_j}{R_i + R_j}} h_{ij}^{1/2}, \mu |\mathbf{F}^\perp| \right) \frac{-\mathbf{v}_{ij}^\parallel}{|\mathbf{v}_{ij}^\parallel|} \quad (8)$$

G_i is the shear modulus of the material and μ is the static friction coefficient. δs is the integrated slip in the shearing direction since the particles first came into contact. δs is allowed to increase until the shearing force exceeds the limit imposed by the static friction. At that point the contact slips and δs is reset to zero.

Walton and Braun [8] were the first who attempted to incorporate Mindlin's friction theory into their simulations using what they called the "incrementally slipping friction model". Their model is computationally more expensive than eq. 8, however, the qualitative results appear to be the same.

When there exist a relative rotation about the axis perpendicular to the contact surface, then the frictional forces will induce a moment to counteract this rotation. In Mindlin's theory this induced moment is described by the following equation when partial slipping is ignored:

$$M_{ij}^{\text{couple}} = \min \left(\frac{8}{3} \frac{G_i G_j \delta \alpha}{G_i (2 - \nu_j) + G_j (2 - \nu_i)} \left[\frac{R_i R_j}{R_i + R_j} \right]^{3/2} h_{ij}^{3/2}, \frac{3\pi}{16} \sqrt{\frac{R_i R_j}{R_i + R_j}} h_{ij}^{1/2} \mu |\mathbf{F}^\perp| \right) [-\text{sign}(\omega^\perp)] \quad (9)$$

ω^\perp is the velocity about the axis perpendicular to the contact surface. $\delta \alpha$ is the integrated angular slip. It plays the same role as δs does for slip along the shear direction.

2.5 The Complete Model

In addition to the couple describe by eq. 9 there will be torques induced by the action of the shear forces, given in eq. 8. $\mathbf{F}_{ij}^{\text{elastic}}$, $\mathbf{F}_{ij}^{\text{viscos}}$ and $\mathbf{F}_{ij}^{\text{meso}}$ do not produce any torques because they act radially.

In total, the model described here depends upon eight material parameters. (In addition to the seven identified above, the density of the material making up the particles is needed in order to calculate the masses used for integrating Newton's equations of motion.) Although all of these parameters are in principle measurable, their determination may, in some cases, be problematic. Measuring the internal viscosities, for example, is a difficult task. Fortunately, it is not necessary to know these parameters to high accuracy in order to obtain good results from the simulations.

2.6 A Note On the Algorithm

The computational procedure used here is a generalization of the molecular dynamics method and consists of calculating the positions and velocities of each particle at every time step [13]. As a prerequisite the forces acting between all pairs of particles must be calculated using the procedure described in the proceeding section. The resulting forces are then employed to integrate the Hamiltonian form of Newton's equations of motion.

Modern workstations, and modern parallel computers, are moving to cache based systems in order to overcome the ever increasing gap between processor speed and memory speed. Using such systems in an efficient manner poses a different set of problems compared to those faced when using vector machines. In particular data locality and cache reuse are the major concerns on cache based systems.

The algorithm used in the present studies attempts to addresses these issues. A complete description of the program will be given elsewhere, here it suffices to mention the program's efficiency in terms of its execution speed on various platforms.

By way of comparison, one of the fastest 2-D programs mentioned in the literature runs at 28.2 Kups (thousands of particle updates per second) on a Sun Sparc-10 [14]. That 2-D program was ported to a Sparc-10 after having been optimized for a vector machine. By comparison, the present 3-D program was optimized for data locality and cache reuse and the speed

processor	Speed (Kups)
Sparc-10	24.1
Sparc-20	37.5
SG R4400	41.3
IBM-Power2	45.2

Table 1: This table gives the program speed (in thousands of particle updates per second) on various processors. For these test, a dense system consisting of 9261 particles in a 3-D cube with periodic boundary conditions on all sides was used.

is given in table 1.

3 Description of the Experiment

The diffusional processes inside a rotating drum can be studied using an arrangement first suggested by Hogg et al. [2]: A drum oriented parallel to the ground is partially filled with two types of distinguishable particles. One type in the left half and one type in the right half as shown in fig. 1

As the drum rotates about its axis at a constant speed, momentum is imparted to the particles in the plane perpendicular to the axis of rotation. Motion along the longitudinal direction occurs only through random momentum changes induced by collisions between particles. Hence, motion parallel to the axis of rotation is diffusive.

The diffusion equation for the concentration of each component can be written as:

$$\frac{\partial C_1(z, \mathcal{N})}{\partial \mathcal{N}} = D \frac{\partial^2 C_1(z, \mathcal{N})}{\partial z^2}, \quad (10)$$

where the natural definition of time for this system has been used, namely: the number of revolutions, \mathcal{N} . $C_1(z, \mathcal{N})$ is the concentration of component 1 along the rotation axis.

Eq. 10 can be solved subject to particle conservation and to the initial condition discussed above, yielding [2]:

$$C_1(z, \mathcal{N}) = \frac{1}{2} + \frac{2}{\pi} \sum_{n=1}^{\infty} \frac{1}{2n-1} \exp \left[-\frac{(2n-1)^2 \pi^2 D \mathcal{N}}{L^2} \right] \sin \left[\frac{(2n-1) \pi z}{L} \right] \quad (11)$$

A similar result is obtained for the second component. In the computer simulations the average location of all the particles belonging to a particular component can be measured with a higher accuracy than the particle concentration as a function of position. From eq. 11, the average position is:

$$\langle z \rangle_1 = \frac{8L}{\pi^3} \sum_{n=1}^{\infty} \frac{(-1)^{n+1}}{(2n-1)^3} \exp \left[-\frac{(2n-1)^2 \pi^2 D \mathcal{N}}{L^2} \right] \quad (12)$$

$$\approx \frac{8L}{\pi^3} \exp \left[-\frac{\pi^2 D \mathcal{N}}{L^2} \right] \quad (13)$$

Eq. 13 is a good approximation to eq. 12. It can easily be checked that all the higher order terms together contribute only about 3% to the average at $\mathcal{N} = 0$. For larger \mathcal{N} , the higher order terms become completely negligible. Hence, by measuring $\langle z \rangle$ as a function of \mathcal{N} one can via eq. 13 obtain the diffusion constant, D .

The computer experiments make use of soft spheres, i.e., particles with an elastic modulus, $E \sim 10^6 \text{ N/m}^2$. It is possible to actually manufacture and use particles with such low elastic moduli in laboratory experiments [6]. Indeed they are valuable for studying inter-particle interactions. The purpose of using them in the present simulations is to save computer time, since the integration time step must be smaller than the collision time which varies like $t_c \sim \sqrt{m/E}$ [5] for particles of mass m . Using a normal value of $E \approx 10^{11}$ would have increased the cpu time 300-fold.

Table 2 list the material parameters and table 3 list the tribological parameters used in the present simulations. As can be seen the softness of the particles is reflected not only in the elastic modulus, but also in the internal viscosities.

The walls of the mixer are also composed of particles in order to reduce the complexity of the force calculation. In the present simulations material-3

Parameter	Material-1	Material-2	Material-3
E	$1.0 \times 10^6 \text{ N/m}^2$	$1.0 \times 10^6 \text{ N/m}^2$	$1.0 \times 10^6 \text{ N/m}^2$
G	$0.3 \times 10^6 \text{ N/m}^2$	$0.3 \times 10^6 \text{ N/m}^2$	$0.3 \times 10^6 \text{ N/m}^2$
ν	0.25	0.25	0.25
ξ	5000 poises	5000 poises	5000 poises
η	5000 Poises	5000 poises	5000 Poises
ρ	1000 kg/m ³	1000 kg/m ³	1000 kg/m ³
R	0.0036 m	0.0024 m	0.0030 m

Table 2: Material parameters used for the soft spheres in the present simulations. (See the text for an explanation of the symbols.)

Parameter	1 - 1	1 - 2	2-2	1-3, 2-3, 3-3
μ	0.1	0.2	0.5	0.2
W	0.2 J/m ²	0.2 J/m ²	0.2 J/m ²	0.2 J/m ²

Table 3: Tribological parameters used for the soft spheres in the present simulations. $i-j$ indicates the value the parameter takes when a particle of material type i is in contact with a particle of material type j . (See the text for an explanation of the symbols.)

was used exclusively for the drum walls and materials 1& 2 where used for the particles inside the drum.

Note, the difference in μ for the three materials. Previous experimental studies of rotating drums indicate that materials with significantly different angles of repose, may segregate rather than mix during the course of the experiment [4]. In the simulations, differences in the angle of repose are achieved by varying either μ , the coefficient of static friction or by varying W , the surface energy. Since common experiments use mixtures of sand and glass beads, varying μ , while keeping W constant should yield results which are more readily comparable with experiments.

The cylindrical drum used in the present simulations was 12 cm long and 8 cm in diameter, giving an aspect ratio of 1.5. At the beginning of the simulation, equal masses of particles from materials 1 or 2 were placed in the drum as described above. The drum was then rotated at a constant angular speed. A typical simulation involved about 1000 particles inside the drum and 1000 particles making up the drum walls.

4 Results and Discussion

As a first step the self-diffusion for particles composed of material 1 is studied. (This is done by giving each particle a tag corresponding to that half of the drum in which it started.) The average position in the longitudinal direction (denoted by: z) is plotted in fig. 2 as a function of the number of drum revolutions for two different rotation speeds. As to be expected, the particles diffused faster at higher rotation speeds.

A further understanding of the diffusion process can be obtained by studying animated videos of the rotating drum. The videos show quite clearly that diffusion is initiated at the free surface of the granulate, diffusion in the bulk plays a subordinate role for the case of a single species. Basically, particles brought up to the free surface via the action of the drum's rotation execute a random walk parallel to the axis of rotation as they roll along the surface.

From fig. 2 and similar plots the diffusion constants can be extracted. A plot of the self-diffusion coefficient as a function of rotation speed is shown in fig. 3. This data agrees qualitatively with the experimental results of Rao et al. [3]. Quantitative agreement is not expect because Rao et al. are using particles with different material properties.

The case of two diffusing species has not, to our knowledge, been studied experimentally. Fig. 4 depicts the average position of the particles composed of material 1 as they diffuse through particles composed of material 2. Note the qualitative difference between this figure and fig. 2. For the two-species situation, the diffusion rate is nearly the same for the two rotation speeds and in fact it is slightly smaller at the higher rotation rate. This counterintuitive phenomenon exists over a range of rotation speeds as illustrated in 5.

Again, animated videos shed some light on the processes taking place. Since the particles of material 2 have a larger coefficient of static friction than those of material 1, their angle of repose is larger, which means that they will tend to roll downhill onto the particles of material 1. The particles of material 2 are also smaller than those of material 1, hence they are able to diffuse through material 1 not only at the surfaces, but also in the bulk. (As layers of species 1 move past each other they open up voids through which the smaller particles can move.) For the two-species case, diffusion in the bulk plays a larger role than for the single-species case.

Another indicator of the enhanced mobility of the smaller particles is given by the ratio of the total kinetic energy of the small particles to that of the larger particles. Fig. 6 shows this ratio as a function of the rotation speed. The solid line indicates the expected ratio if the average velocity of particles belonging to both species were equal. As can be seen, the measured ratios lie above this line, thus the smaller particles are moving, on average, with higher speeds than the larger particles. In other words, the diffusion in this two-component system is being driven by the smaller particles.

At larger rotation speeds particles roll down the surface faster leaving less time for motion parallel to the rotation axis. Hence, the diffusion processes are slowed because there are fewer particles from species 2 rolling onto those of species 1. Eventually, as the rotation speed increases, the entire free surface will fluidize allowing for increased mobility in the longitudinal direction and the diffusion coefficient increases.

If the rotation speed is increased still further, one eventually enters the centrifugal regime where the particles are held to the inner surface of the drum via centrifugal forces. In this regime all diffusion must come to a halt. This implies that there must be a maximum diffusion coefficient at some rotation speed larger than those which could be studied here.

Likewise, as the rotation speed decreases towards zero the mobility of the small particles must also decrease until the diffusive motion stops, conse-

quently, there must also be a maximum diffusion coefficient at some rotation speed much smaller than those which could be studied here.

5 Summary and Conclusions

A computational model for the collision of two visco-elastic spheres which is independent of arbitrary parameters has been presented. Using this model the diffusion of particles in a three dimensional rotating drum has been studied. The major result is that the diffusion coefficient for a two-component system has a much richer structure than anticipated by studying a single-component system. This is primarily due to the larger mobility of the smaller particles compared to that of the larger particles.

One phenomena in rotating drums which has been given a good deal of attention in the literature is the spontaneous segregation of two material types [4]. In a typical experiment, one component is smaller and rougher (and thus has a larger angle of repose) than the other. After about 5 minutes of rotation, the two materials spontaneously segregate into a series of bands parallel to the rotation axis. The composition of the bands alternates between high concentrations of component 1 and high concentrations of component 2. In most cases there is an odd number of bands, with the smaller, rougher particles located at the ends of the drums.

The mechanisms which create this banded structure are fairly well understood. A statistical fluctuation in the concentration of the smaller, rougher component yields a local increase in the angle of repose. The larger particles will tend to roll away from such a locality, thus depleting their numbers in the region of the fluctuation which drives the angle of repose to even higher values. Now, it is not completely understood why the bands should be stable, since as shown here, particle diffusion will tend to destroy the banded pattern.

This phenomena occurs on a time scale which is too large to be simulated with present resources, however, the above results can be applied to this problem. The present work has shown that diffusion in two-component systems is driven by the mobility of the smaller particles. Therefore it is possible to understand the stability of band patterns as follows. Let a band of large particles exist between two bands of smaller particles. If the rate at which the small particles diffuse through the larger particles is large enough,

then the small particles from one band can diffuse through the band of large particles and replenish the band of small particles on the other side. Now if the current of small particles is conserved, then diffusion of the large particles into the region occupied by the small particles will be depressed due to geometrical factors.

This idea implies that only systems with an odd number of bands are stable, as is indeed reported in the literature. (There has been only one reported experiment yielding an even number of bands [4], however they did not use a simple cylindrical drum, rather they used a more complicated drum shape which enhanced the angle of repose of the larger particles.) Furthermore it explains why early experiments claimed that the segregation started with the smaller particles at the ends of the drum. Indeed any other arrangement would necessarily be unstable.

It may be possible to test these and other ideas on spontaneous material segregation in the near future through the use of high performance computer systems.

References

- [1] O.R. Walton and R.L. Braun, *Proceedings of DOE/NSF Workshop on Flow of Particulates and Fluids* (Ithaca, NY 1993). G.H. Ristow, *Euro. Phys. Lett.* **28** (1994) 97. G. Baumann, I.M. Jánosi and D.E. Wolf, *Phys. Rev.* **E51** (1995) 1879.
- [2] R. Hogg, D.S. Cahn, T.W. Healy and D.W. Feurstenau, *Chem. Eng. Sci.* **21** (1966) 1025.
- [3] S.J. Rao, S.K. Bhatia and D.V. Khakhar, *Powder Techn.* **67** (1991) 153.
- [4] M.B. Donald and B. Roseman, *British Chem. Eng.* **7** (1962) 749. A.R. Rogers and J.A. Clements, *Powder Techn.* **5** (1971) 167. O. Zik, D. Levine, S.G. Lipson, S. Shtrikman and J. Stavans, *Phys. Rev. Lett.* **73** (1994) 644.
- [5] H. Hertz, *Gesammelte Werke*, (Leipzig, 1895). L. D. Landau and E. M. Lifschitz, *Course of Theoretical Physics, Theorie of Elasticity Vol. 7*, (Pergamon Press, London 1959). K.L. Johnson, *Brit. J. Appl. Phys.* **9**, 199 (1958).
- [6] K.L. Johnson, K. Kendall and A.D. Roberts, *Proc. R. Soc. Lond. A.* **324**, 301 (1971).
- [7] G. Kuwabara and K. Kono, *Jap. J. App. Phys.* **26**, 1230 (1971).
- [8] R.D. Mindlin, *J. App. Mech.* **16**, 259 (1949).
- [9] H.C. Hamaker, *Physica IV* **10**, 1058 (1937).
- [10] B. Dahneke, *J. Colloid and Interface Sci.* **40**, 1 (1972).
- [11] G.A. Kohring, *J. Phys. I (France)* **4**, 1779 (1994).
- [12] O.R. Walton and R.L. Braun, *J. Rheology* **30**, 949 (1986).
- [13] P.A. Cundall and O.D.L. Strack, *Geotech.* **29**, 47 (1979). M. P. Allen and D. J. Tildesley, *Computer Simulations of Liquids*, (Clarendon Press, Oxford 1987).
- [14] W. Form, N. Ito and G.A. Kohring, *Int. J. Mod. Phys. C* **4**, 1085 (1993).

6 Figures

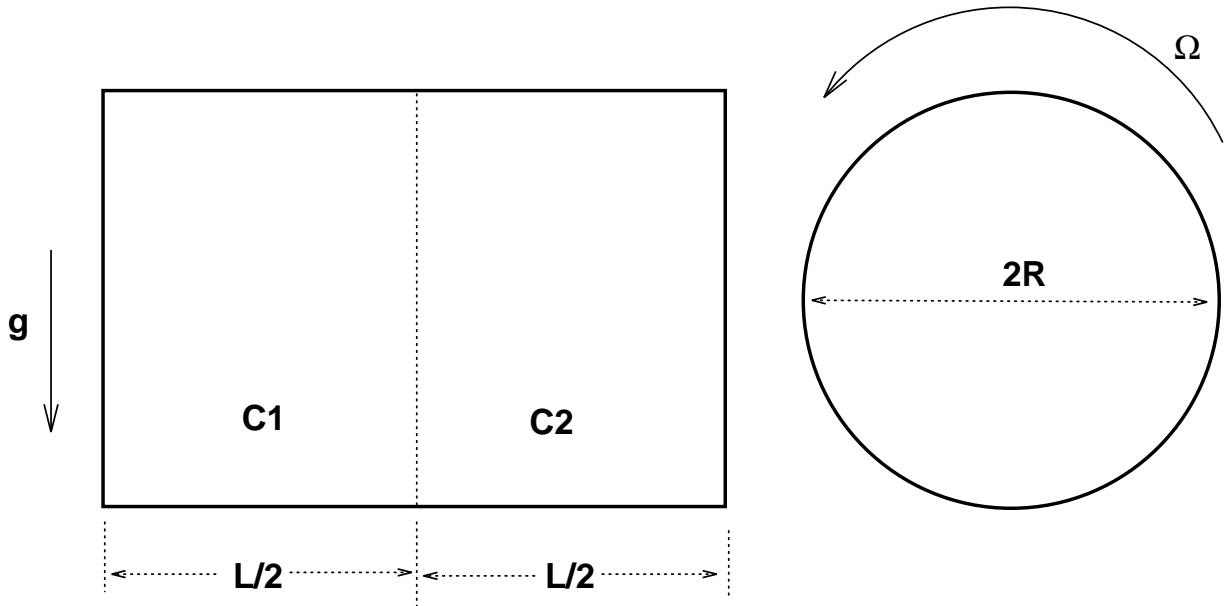


Figure 1: Schematic illustrating the experimental set-up. Initially the two material components, C1 and C2 are well separated.

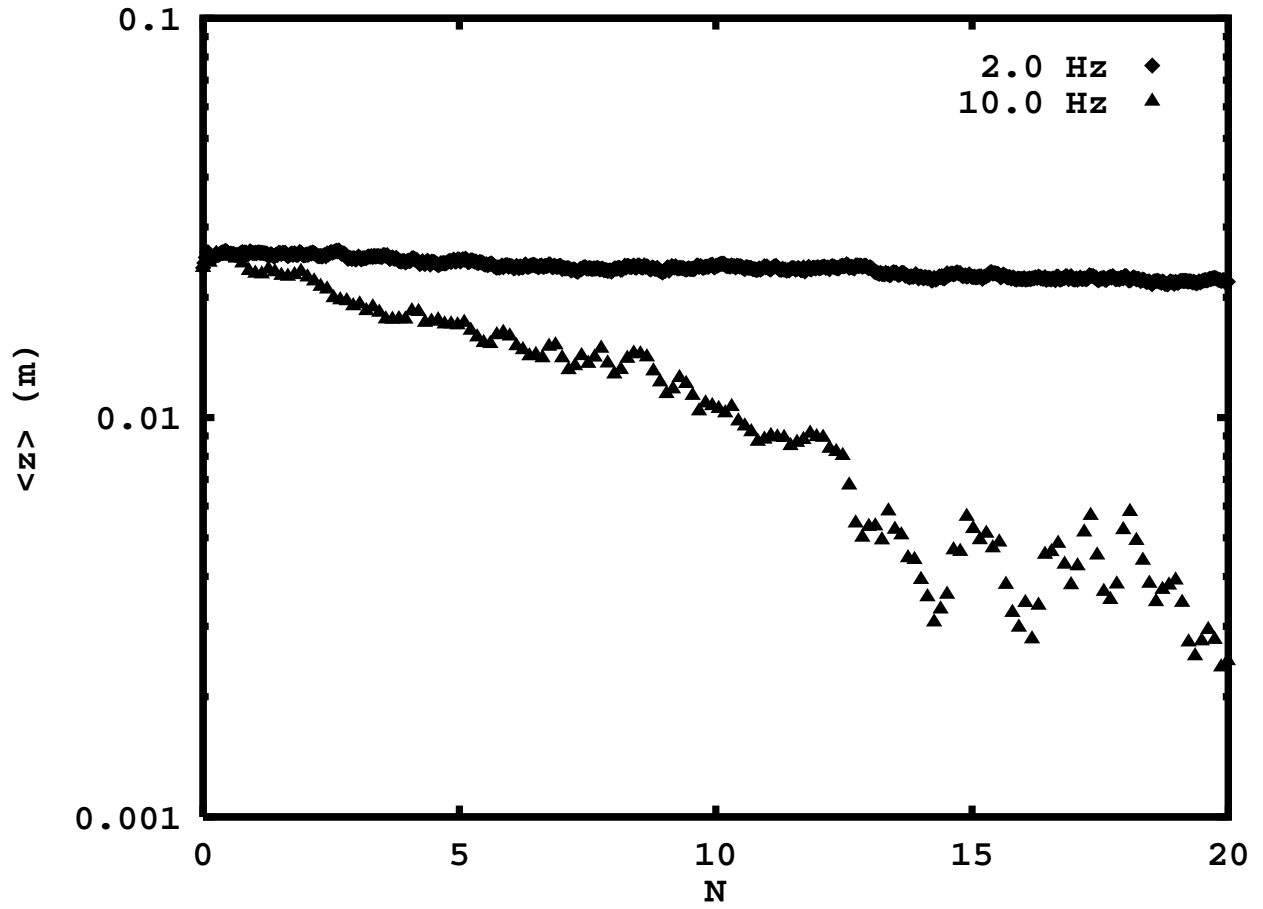


Figure 2: Self-diffusion: Average position as a function of the number of revolutions \mathcal{N} for two different rotation speeds.

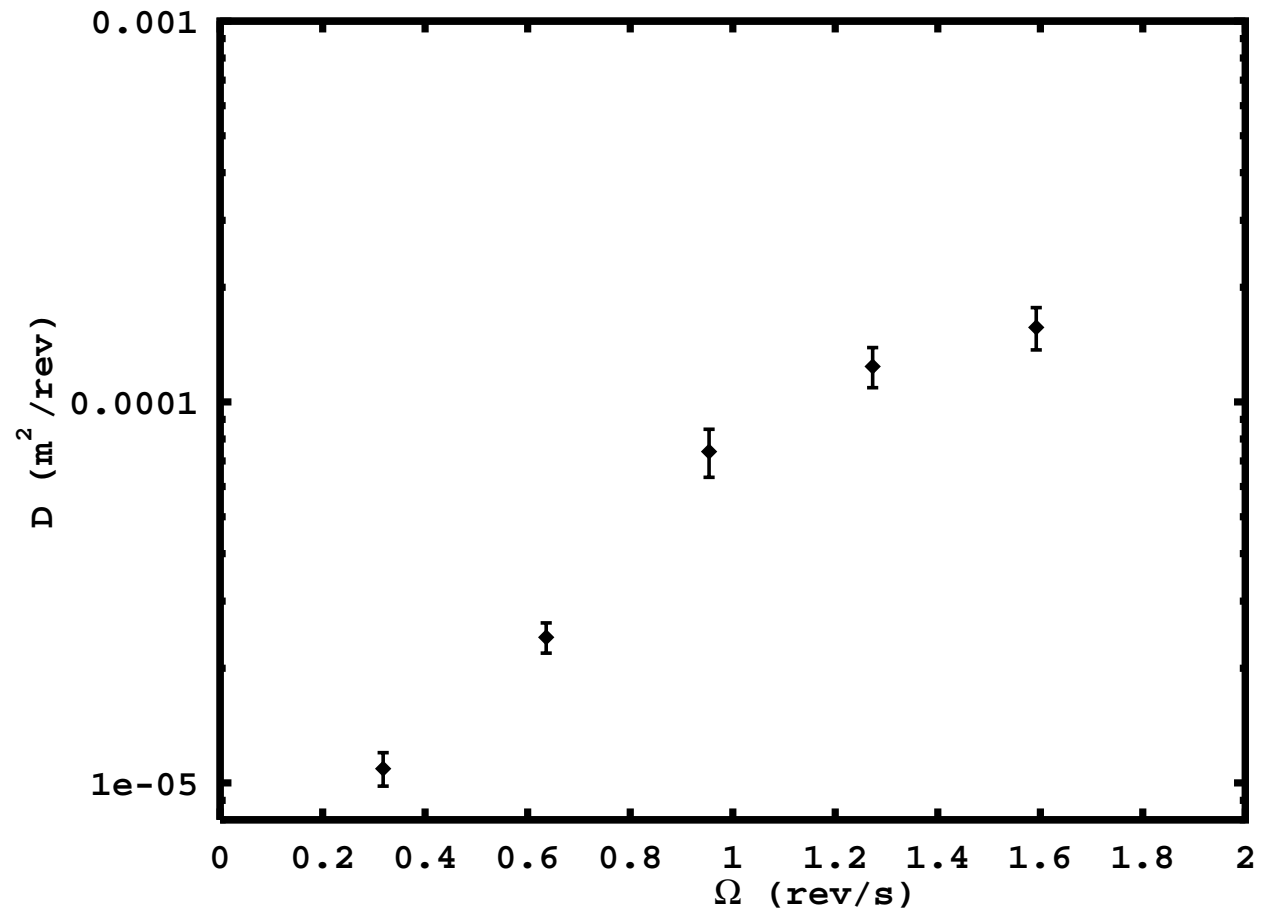


Figure 3: Diffusion coefficients for self-diffusion as a function of the number of revolutions.

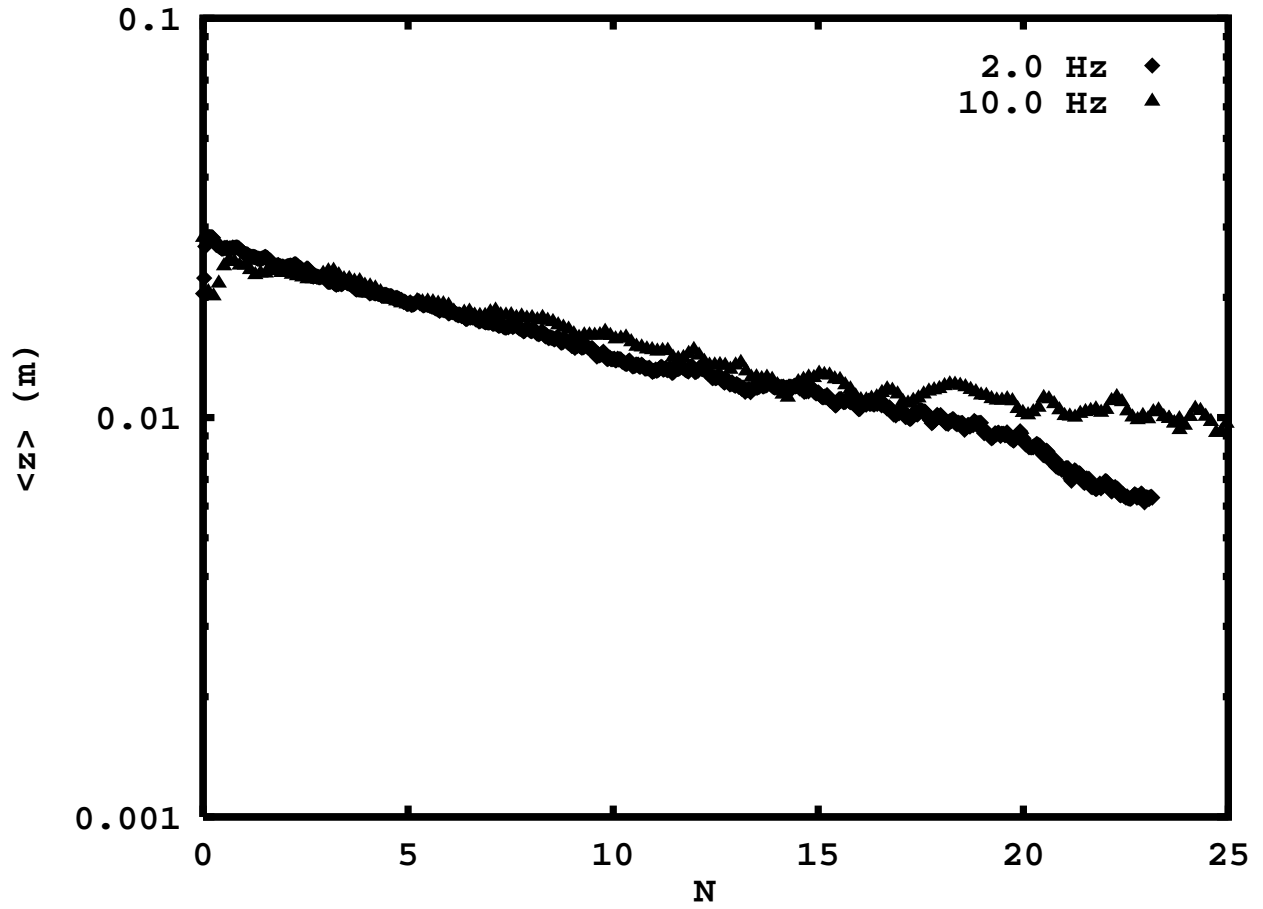


Figure 4: 2-Component diffusion: Average position as a function of the number of revolutions \mathcal{N} for two different rotation speeds.

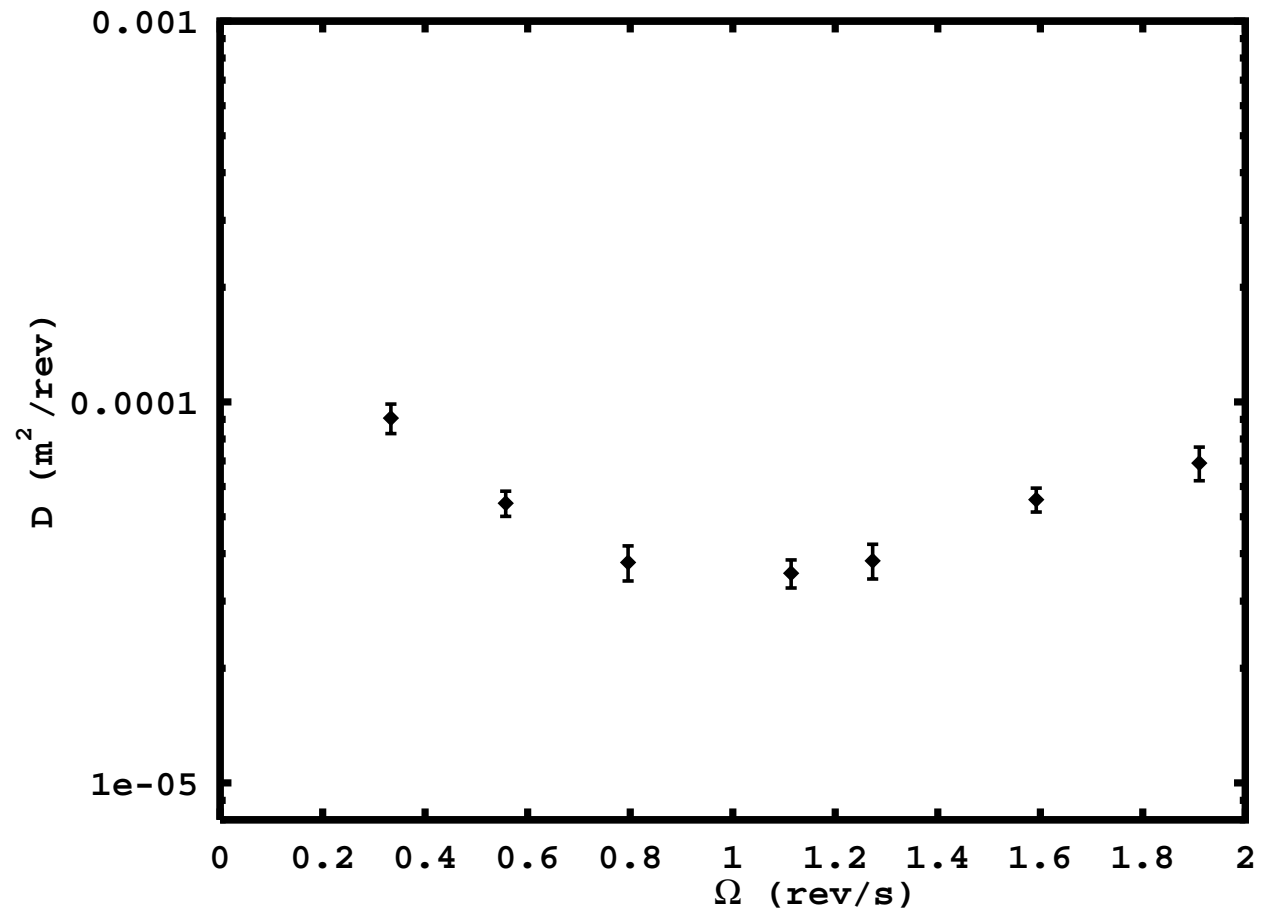


Figure 5: Diffusion coefficients for 2-component diffusion as a function of the number of revolutions.

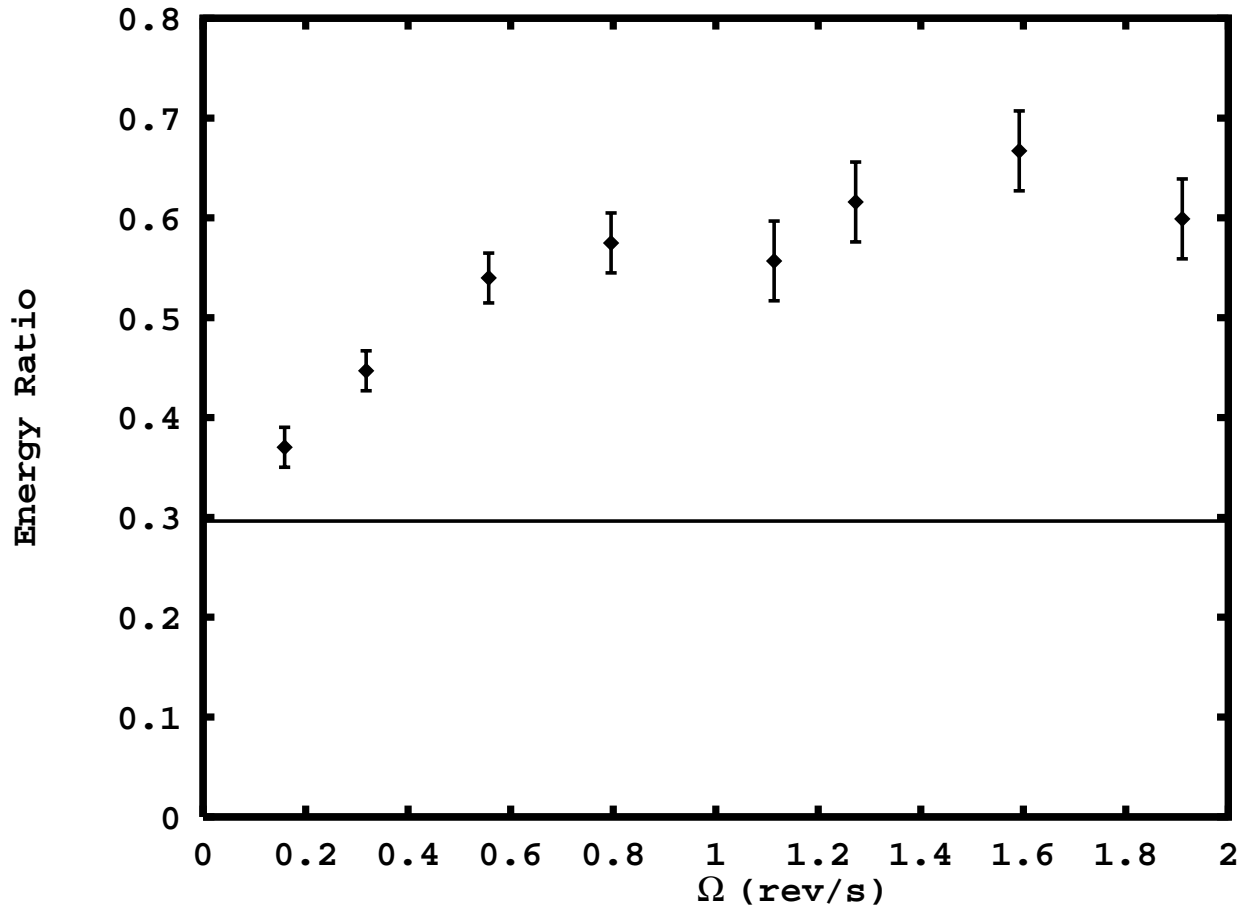


Figure 6: The ratio of the average kinetic energy for particles composed of material 2 to that for particles composed of material 1.

Studies of Diffusional Mixing in Rotating Drums via Computer Simulations

G.A. Kohring

Central Institute for Applied Mathematics

Research Center Jülich (KFA)

D-52425 Jülich, Germany

g.kohring@kfa-juelich.de

Abstract

Particle diffusion in rotating drums is studied via computer simulations using a full 3-D model which does not involve any arbitrary input parameters. The diffusion coefficient for single-component systems agree qualitatively with previous experimental results. On the other hand, the diffusion coefficient for two-component systems is shown to be a highly nonlinear function of the rotation velocity. It is suggested that this results from a competition between the diffusive motion parallel to, and flowing motion perpendicular to the axis of rotation.

(submitted to *Journal de Physique*)

1 Introduction

Rotating drums perform critical functions in many industrial processes. They are utilized for tasks such as humidification, dehumidification, convective heat transfer, facilitation of gas-solid catalytic reactions and, not the least, ordinary mixing or blending. Understanding the mechanisms behind particle

mobility in rotating drums is an important step towards refining the efficiency of such processes. In the absence of mechanical agitators, momentum is imparted to the particles only in the plane perpendicular to the rotation axis. Motion parallel to the axis of rotation occurs through momentum changes induced by the collisions between particles. Since these collisions occur more or less randomly in time, this motion is diffusive in nature. Until now most computer simulations have neglected the essential three-dimensional character of these systems and, via two-dimensional simulations, concentrated on the motion perpendicular to the rotation axis [1]. In the present work the diffusive motion in the longitudinal direction is examined using a full three-dimensional model.

Previous experimental studies of diffusive motion in rotating cylinders have concentrated on single-component systems, i.e., a cylinder partially filled with a single particle type [2, 3]. One-half of the particles were dyed a different color in order to make them distinguishable. These diffusion experiments were simplified through the use of an ideal starting arrangement: initially, the colored particles are axially segregated so that mixing occurs only through the diffusive motion parallel to the rotation axis. Under these ideal circumstances, some aspects of the diffusive mixing can be studied analytically and Hogg et al. [2] obtained good agreement between the theory and experiment.

The present study focuses on diffusion in two-component systems. Diffusion in two-component systems is expected to exhibit characteristics not found in single-component systems, because the former have been shown to exhibit spontaneous material segregation [4]. In this form of segregation several bands parallel to the rotation axis are formed. These bands alternate between the two material types and there is normally an odd number of such bands. The nature of this phenomena is not completely understood, however, it is clear that diffusion must play an important role. Indeed the results to be presented here demonstrate a distinct difference between the diffusion in 1-component and 2-component systems.

In the following section, a three dimensional model for colliding, visco-elastic spheres is presented and its numerical implementation is discussed. The next section describes the experimental arrangement. Following that, the results are presented and discussed. The paper concludes with some speculative comments on the mechanisms behind material segregation in rotation drums.

2 A Computational Model for Visco-Elastic, Mesoscopic, Spherical Particles

The contact-force model presented here is based upon a visco-elastic model for the collision of two mesoscopic, spherical particles developed over the last 100 years by Hertz [5], Johnson et al. [6], Kuwabara and Kono [7] and Mindlin [8]. This model is free of arbitrary parameters in the sense that all input variables are material properties amenable to experimental verification. The model involves four key elements: 1) particle elasticity, 2) energy loss through internal friction, 3) attraction on the contact surface and 4) energy loss through the action of frictional forces.

2.1 Particle Elasticity

As demonstrated by H. Hertz [5], the deformation of elastic particles of finite extent leads to a nonlinear dependence between the compressive force and the compression length.

$$\mathbf{F}_{ij}^{\text{elastic}} = \frac{4}{3} \frac{E_i E_j}{E_i (1 - \nu_j^2) + E_j (1 - \nu_i^2)} \sqrt{\frac{R_i R_j}{R_i + R_j}} h_{ij}^{3/2} \mathbf{n}_{ij}^{\perp}, \quad (1)$$

where,

$$h_{ij} = R_i + R_j - |\mathbf{X}_i - \mathbf{X}_j|, \quad (2)$$

and,

$$\mathbf{n}_{ij} = \frac{\mathbf{X}_i - \mathbf{X}_j}{|\mathbf{X}_i - \mathbf{X}_j|}. \quad (3)$$

Here, R_i symbolizes the radius of the i -th particle. E_i represents the elastic modulus and ν_i the Poisson ratio. \mathbf{X}_i is the position vector of the i -th particle and \mathbf{n}_{ij}^{\perp} indicates a unit vector pointing from grain j to grain i perpendicular to the contact surface. (Because all the forces described here are contact forces, they are nonzero only if $h_{ij} > 0$.)

2.2 Internal Friction

Energy dissipation due to the viscous nature of the solid particles was first studied by Kuwabara and Kono [7] more than a century after Hertz's work.

They obtained the following expression for the non-conservative viscous force acting during a collision:

$$\mathbf{F}_{ij}^{\text{viscos}} = -2 \frac{B_i B_j}{B_i (1 - \sigma_j^2) + B_j (1 - \sigma_i^2)} \sqrt{\frac{R_i R_j}{R_i + R_j}} h_{ij}^{1/2} \mathbf{v}_{ij}^{\perp}, \quad (4)$$

where,

$$B_i = \frac{9\xi_i\eta_i}{3\xi_i + \eta_i} \quad (5)$$

and,

$$\sigma_i = \frac{3\xi_i - 3\eta_i}{2(3\xi_i + \eta_i)}. \quad (6)$$

ξ_i and η_i are the coefficients of viscosity associated with volume deformation and shear. \mathbf{v}_{ij}^{\perp} is the relative velocity of the colliding particles normal to the contact surface.

2.3 Surface Attraction

When two surfaces are brought into contact an attractive force due to the attractive part of the inter-molecular interaction arises. The case of spherical particles composed of molecules interacting via a Lennard-Jones potential was first studied by Hamaker [9] for non-elastic grains. It was extended to the case of elastic grains by Dahneke [10]. The form used here was introduced by Johnson et al. [6] for a general molecular interaction characterized by the surface energy, W_{ij} , of the contacting materials.

$$\mathbf{F}_{ij}^{\text{meso}} = -\sqrt{\frac{4}{3} \frac{8\pi W_{ij} E_i E_j}{E_i (1 - \nu_j^2) + E_j (1 - \nu_i^2)}} \left(\frac{R_i R_j}{R_i + R_j}\right)^{1/4} h_{ij}^{3/4} \mathbf{n}_{ij}^{\perp} \quad (7)$$

Note the small power, 1/4, to which the reduced radius is raised. Since the weight of a spherical grain is equal to $4/3\pi\rho g R^3$, there will be a grain size for which the weight of a particle is equal in magnitude to this attractive force. Particles smaller than this critical size experience this interaction as an adhesive. Typically, this critical grain size is on the order of 1 mm [11]. For grain sizes much larger than about 1 cm, this force can be neglected.

2.4 External Friction Forces

The frictional forces which develop under conditions of slip parallel to, or rotation about the normal to the contact surface were first studied by Mindlin [8]. Mindlin's original expression is computationally expensive, therefore a simplified expression is used which amounts to assuming that no partial slipping of the contact surfaces occurs.

$$\mathbf{F}_{ij}^{\text{shear}} = \min \left(\frac{16}{3} \frac{G_i G_j \delta s}{G_i (2 - \nu_j) + G_j (2 - \nu_i)} \sqrt{\frac{R_i R_j}{R_i + R_j}} h_{ij}^{1/2}, \mu |\mathbf{F}^\perp| \right) \frac{-\mathbf{v}_{ij}^\parallel}{|\mathbf{v}_{ij}^\parallel|} \quad (8)$$

G_i is the shear modulus of the material and μ is the static friction coefficient. δs is the integrated slip in the shearing direction since the particles first came into contact. δs is allowed to increase until the shearing force exceeds the limit imposed by the static friction. At that point the contact slips and δs is reset to zero.

Walton and Braun [8] were the first who attempted to incorporate Mindlin's friction theory into their simulations using what they called the "incrementally slipping friction model". Their model is computationally more expensive than eq. 8, however, the qualitative results appear to be the same.

When there exist a relative rotation about the axis perpendicular to the contact surface, then the frictional forces will induce a moment to counteract this rotation. In Mindlin's theory this induced moment is described by the following equation when partial slipping is ignored:

$$M_{ij}^{\text{couple}} = \min \left(\frac{8}{3} \frac{G_i G_j \delta \alpha}{G_i (2 - \nu_j) + G_j (2 - \nu_i)} \left[\frac{R_i R_j}{R_i + R_j} \right]^{3/2} h_{ij}^{3/2}, \frac{3\pi}{16} \sqrt{\frac{R_i R_j}{R_i + R_j}} h_{ij}^{1/2} \mu |\mathbf{F}^\perp| \right) [-\text{sign}(\omega^\perp)] \quad (9)$$

ω^\perp is the velocity about the axis perpendicular to the contact surface. $\delta \alpha$ is the integrated angular slip. It plays the same role as δs does for slip along the shear direction.

2.5 The Complete Model

In addition to the couple describe by eq. 9 there will be torques induced by the action of the shear forces, given in eq. 8. $\mathbf{F}_{ij}^{\text{elastic}}$, $\mathbf{F}_{ij}^{\text{viscos}}$ and $\mathbf{F}_{ij}^{\text{meso}}$ do not produce any torques because they act radially.

In total, the model described here depends upon eight material parameters. (In addition to the seven identified above, the density of the material making up the particles is needed in order to calculate the masses used for integrating Newton's equations of motion.) Although all of these parameters are in principle measurable, their determination may, in some cases, be problematic. Measuring the internal viscosities, for example, is a difficult task. Fortunately, it is not necessary to know these parameters to high accuracy in order to obtain good results from the simulations.

2.6 A Note On the Algorithm

The computational procedure used here is a generalization of the molecular dynamics method and consists of calculating the positions and velocities of each particle at every time step [13]. As a prerequisite the forces acting between all pairs of particles must be calculated using the procedure described in the proceeding section. The resulting forces are then employed to integrate the Hamiltonian form of Newton's equations of motion.

Modern workstations, and modern parallel computers, are moving to cache based systems in order to overcome the ever increasing gap between processor speed and memory speed. Using such systems in an efficient manner poses a different set of problems compared to those faced when using vector machines. In particular data locality and cache reuse are the major concerns on cache based systems.

The algorithm used in the present studies attempts to addresses these issues. A complete description of the program will be given elsewhere, here it suffices to mention the program's efficiency in terms of its execution speed on various platforms.

By way of comparison, one of the fastest 2-D programs mentioned in the literature runs at 28.2 Kups (thousands of particle updates per second) on a Sun Sparc-10 [14]. That 2-D program was ported to a Sparc-10 after having been optimized for a vector machine. By comparison, the present 3-D program was optimized for data locality and cache reuse and the speed

processor	Speed (Kups)
Sparc-10	24.1
Sparc-20	37.5
SG R4400	41.3
IBM-Power2	45.2

Table 1: This table gives the program speed (in thousands of particle updates per second) on various processors. For these test, a dense system consisting of 9261 particles in a 3-D cube with periodic boundary conditions on all sides was used.

is given in table 1.

3 Description of the Experiment

The diffusional processes inside a rotating drum can be studied using an arrangement first suggested by Hogg et al. [2]: A drum oriented parallel to the ground is partially filled with two types of distinguishable particles. One type in the left half and one type in the right half as shown in fig. 1

As the drum rotates about its axis at a constant speed, momentum is imparted to the particles in the plane perpendicular to the axis of rotation. Motion along the longitudinal direction occurs only through random momentum changes induced by collisions between particles. Hence, motion parallel to the axis of rotation is diffusive.

The diffusion equation for the concentration of each component can be written as:

$$\frac{\partial C_1(z, \mathcal{N})}{\partial \mathcal{N}} = D \frac{\partial^2 C_1(z, \mathcal{N})}{\partial z^2}, \quad (10)$$

where the natural definition of time for this system has been used, namely: the number of revolutions, \mathcal{N} . $C_1(z, \mathcal{N})$ is the concentration of component 1 along the rotation axis.

Eq. 10 can be solved subject to particle conservation and to the initial condition discussed above, yielding [2]:

$$C_1(z, \mathcal{N}) = \frac{1}{2} + \frac{2}{\pi} \sum_{n=1}^{\infty} \frac{1}{2n-1} \exp \left[-\frac{(2n-1)^2 \pi^2 D \mathcal{N}}{L^2} \right] \sin \left[\frac{(2n-1) \pi z}{L} \right] \quad (11)$$

A similar result is obtained for the second component. In the computer simulations the average location of all the particles belonging to a particular component can be measured with a higher accuracy than the particle concentration as a function of position. From eq. 11, the average position is:

$$\langle z \rangle_1 = \frac{8L}{\pi^3} \sum_{n=1}^{\infty} \frac{(-1)^{n+1}}{(2n-1)^3} \exp \left[-\frac{(2n-1)^2 \pi^2 D \mathcal{N}}{L^2} \right] \quad (12)$$

$$\approx \frac{8L}{\pi^3} \exp \left[-\frac{\pi^2 D \mathcal{N}}{L^2} \right] \quad (13)$$

Eq. 13 is a good approximation to eq. 12. It can easily be checked that all the higher order terms together contribute only about 3% to the average at $\mathcal{N} = 0$. For larger \mathcal{N} , the higher order terms become completely negligible. Hence, by measuring $\langle z \rangle$ as a function of \mathcal{N} one can via eq. 13 obtain the diffusion constant, D .

The computer experiments make use of soft spheres, i.e., particles with an elastic modulus, $E \sim 10^6 \text{ N/m}^2$. It is possible to actually manufacture and use particles with such low elastic moduli in laboratory experiments [6]. Indeed they are valuable for studying inter-particle interactions. The purpose of using them in the present simulations is to save computer time, since the integration time step must be smaller than the collision time which varies like $t_c \sim \sqrt{m/E}$ [5] for particles of mass m . Using a normal value of $E \approx 10^{11}$ would have increased the cpu time 300-fold.

Table 2 list the material parameters and table 3 list the tribological parameters used in the present simulations. As can be seen the softness of the particles is reflected not only in the elastic modulus, but also in the internal viscosities.

The walls of the mixer are also composed of particles in order to reduce the complexity of the force calculation. In the present simulations material-3

Parameter	Material-1	Material-2	Material-3
E	$1.0 \times 10^6 \text{ N/m}^2$	$1.0 \times 10^6 \text{ N/m}^2$	$1.0 \times 10^6 \text{ N/m}^2$
G	$0.3 \times 10^6 \text{ N/m}^2$	$0.3 \times 10^6 \text{ N/m}^2$	$0.3 \times 10^6 \text{ N/m}^2$
ν	0.25	0.25	0.25
ξ	5000 poises	5000 poises	5000 poises
η	5000 Poises	5000 poises	5000 Poises
ρ	1000 kg/m ³	1000 kg/m ³	1000 kg/m ³
R	0.0036 m	0.0024 m	0.0030 m

Table 2: Material parameters used for the soft spheres in the present simulations. (See the text for an explanation of the symbols.)

Parameter	1 - 1	1 - 2	2-2	1-3, 2-3, 3-3
μ	0.1	0.2	0.5	0.2
W	0.2 J/m ²	0.2 J/m ²	0.2 J/m ²	0.2 J/m ²

Table 3: Tribological parameters used for the soft spheres in the present simulations. $i-j$ indicates the value the parameter takes when a particle of material type i is in contact with a particle of material type j . (See the text for an explanation of the symbols.)

was used exclusively for the drum walls and materials 1 & 2 were used for the particles inside the drum.

Note, the difference in μ for the three materials. Previous experimental studies of rotating drums indicate that materials with significantly different angles of repose, may segregate rather than mix during the course of the experiment [4]. In the simulations, differences in the angle of repose are achieved by varying either μ , the coefficient of static friction or by varying W , the surface energy. Since common experiments use mixtures of sand and glass beads, varying μ , while keeping W constant should yield results which are more readily comparable with experiments.

The cylindrical drum used in the present simulations was 12 cm long and 8 cm in diameter, giving an aspect ratio of 1.5. At the beginning of the simulation, equal masses of particles from materials 1 or 2 were placed in the drum as described above. The drum was then rotated at a constant angular speed. A typical simulation involved about 1000 particles inside the drum and 1000 particles making up the drum walls.

4 Results and Discussion

As a first step the self-diffusion for particles composed of material 1 is studied. (This is done by giving each particle a tag corresponding to that half of the drum in which it started.) The average position in the longitudinal direction (denoted by: z) is plotted in fig. 2 as a function of the number of drum revolutions for two different rotation speeds. As to be expected, the particles diffused faster at higher rotation speeds.

A further understanding of the diffusion process can be obtained by studying animated videos of the rotating drum. The videos show quite clearly that diffusion is initiated at the free surface of the granulate, diffusion in the bulk plays a subordinate role for the case of a single species. Basically, particles brought up to the free surface via the action of the drum's rotation execute a random walk parallel to the axis of rotation as they roll along the surface.

From fig. 2 and similar plots the diffusion constants can be extracted. A plot of the self-diffusion coefficient as a function of rotation speed is shown in fig. 3. This data agrees qualitatively with the experimental results of Rao et al. [3]. Quantitative agreement is not expected because Rao et al. are using particles with different material properties.

The case of two diffusing species has not, to our knowledge, been studied experimentally. Fig. 4 depicts the average position of the particles composed of material 1 as they diffuse through particles composed of material 2. Note the qualitative difference between this figure and fig. 2. For the two-species situation, the diffusion rate is nearly the same for the two rotation speeds and in fact it is slightly smaller at the higher rotation rate. This counterintuitive phenomenon exists over a range of rotation speeds as illustrated in 5.

Again, animated videos shed some light on the processes taking place. Since the particles of material 2 have a larger coefficient of static friction than those of material 1, their angle of repose is larger, which means that they will tend to roll downhill onto the particles of material 1. The particles of material 2 are also smaller than those of material 1, hence they are able to diffuse through material 1 not only at the surfaces, but also in the bulk. (As layers of species 1 move past each other they open up voids through which the smaller particles can move.) For the two-species case, diffusion in the bulk plays a larger role than for the single-species case.

Another indicator of the enhanced mobility of the smaller particles is given by the ratio of the total kinetic energy of the small particles to that of the larger particles. Fig. 6 shows this ratio as a function of the rotation speed. The solid line indicates the expected ratio if the average velocity of particles belonging to both species were equal. As can be seen, the measured ratios lie above this line, thus the smaller particles are moving, on average, with higher speeds than the larger particles. In other words, the diffusion in this two-component system is being driven by the smaller particles.

At larger rotation speeds particles roll down the surface faster leaving less time for motion parallel to the rotation axis. Hence, the diffusion processes are slowed because there are fewer particles from species 2 rolling onto those of species 1. Eventually, as the rotation speed increases, the entire free surface will fluidize allowing for increased mobility in the longitudinal direction and the diffusion coefficient increases.

If the rotation speed is increased still further, one eventually enters the centrifugal regime where the particles are held to the inner surface of the drum via centrifugal forces. In this regime all diffusion must come to a halt. This implies that there must be a maximum diffusion coefficient at some rotation speed larger than those which could be studied here.

Likewise, as the rotation speed decreases towards zero the mobility of the small particles must also decrease until the diffusive motion stops, conse-

quently, there must also be a maximum diffusion coefficient at some rotation speed much smaller than those which could be studied here.

5 Summary and Conclusions

A computational model for the collision of two visco-elastic spheres which is independent of arbitrary parameters has been presented. Using this model the diffusion of particles in a three dimensional rotating drum has been studied. The major result is that the diffusion coefficient for a two-component system has a much richer structure than anticipated by studying a single-component system. This is primarily due to the larger mobility of the smaller particles compared to that of the larger particles.

One phenomena in rotating drums which has been given a good deal of attention in the literature is the spontaneous segregation of two material types [4]. In a typical experiment, one component is smaller and rougher (and thus has a larger angle of repose) than the other. After about 5 minutes of rotation, the two materials spontaneously segregate into a series of bands parallel to the rotation axis. The composition of the bands alternates between high concentrations of component 1 and high concentrations of component 2. In most cases there is an odd number of bands, with the smaller, rougher particles located at the ends of the drums.

The mechanisms which create this banded structure are fairly well understood. A statistical fluctuation in the concentration of the smaller, rougher component yields a local increase in the angle of repose. The larger particles will tend to roll away from such a locality, thus depleting their numbers in the region of the fluctuation which drives the angle of repose to even higher values. Now, it is not completely understood why the bands should be stable, since as shown here, particle diffusion will tend to destroy the banded pattern.

This phenomena occurs on a time scale which is too large to be simulated with present resources, however, the above results can be applied to this problem. The present work has shown that diffusion in two-component systems is driven by the mobility of the smaller particles. Therefore it is possible to understand the stability of band patterns as follows. Let a band of large particles exist between two bands of smaller particles. If the rate at which the small particles diffuse through the larger particles is large enough,

then the small particles from one band can diffuse through the band of large particles and replenish the band of small particles on the other side. Now if the current of small particles is conserved, then diffusion of the large particles into the region occupied by the small particles will be depressed due to geometrical factors.

This idea implies that only systems with an odd number of bands are stable, as is indeed reported in the literature. (There has been only one reported experiment yielding an even number of bands [4], however they did not use a simple cylindrical drum, rather they used a more complicated drum shape which enhanced the angle of repose of the larger particles.) Furthermore it explains why early experiments claimed that the segregation started with the smaller particles at the ends of the drum. Indeed any other arrangement would necessarily be unstable.

It may be possible to test these and other ideas on spontaneous material segregation in the near future through the use of high performance computer systems.

References

- [1] O.R. Walton and R.L. Braun, *Proceedings of DOE/NSF Workshop on Flow of Particulates and Fluids* (Ithaca, NY 1993). G.H. Ristow, *Euro. Phys. Lett.* **28** (1994) 97. G. Baumann, I.M. Jánosi and D.E. Wolf, *Phys. Rev.* **E51** (1995) 1879.
- [2] R. Hogg, D.S. Cahn, T.W. Healy and D.W. Feurstenau, *Chem. Eng. Sci.* **21** (1966) 1025.
- [3] S.J. Rao, S.K. Bhatia and D.V. Khakhar, *Powder Techn.* **67** (1991) 153.
- [4] M.B. Donald and B. Roseman, *British Chem. Eng.* **7** (1962) 749. A.R. Rogers and J.A. Clements, *Powder Techn.* **5** (1971) 167. O. Zik, D. Levine, S.G. Lipson, S. Shtrikman and J. Stavans, *Phys. Rev. Lett.* **73** (1994) 644.
- [5] H. Hertz, *Gesammelte Werke*, (Leipzig, 1895). L. D. Landau and E. M. Lifschitz, *Course of Theoretical Physics, Theorie of Elasticity Vol. 7*, (Pergamon Press, London 1959). K.L. Johnson, *Brit. J. Appl. Phys.* **9**, 199 (1958).
- [6] K.L. Johnson, K. Kendall and A.D. Roberts, *Proc. R. Soc. Lond. A.* **324**, 301 (1971).
- [7] G. Kuwabara and K. Kono, *Jap. J. App. Phys.* **26**, 1230 (1971).
- [8] R.D. Mindlin, *J. App. Mech.* **16**, 259 (1949).
- [9] H.C. Hamaker, *Physica IV* **10**, 1058 (1937).
- [10] B. Dahneke, *J. Colloid and Interface Sci.* **40**, 1 (1972).
- [11] G.A. Kohring, *J. Phys. I (France)* **4**, 1779 (1994).
- [12] O.R. Walton and R.L. Braun, *J. Rheology* **30**, 949 (1986).
- [13] P.A. Cundall and O.D.L. Strack, *Geotech.* **29**, 47 (1979). M. P. Allen and D. J. Tildesley, *Computer Simulations of Liquids*, (Clarendon Press, Oxford 1987).
- [14] W. Form, N. Ito and G.A. Kohring, *Int. J. Mod. Phys. C* **4**, 1085 (1993).

6 Figures

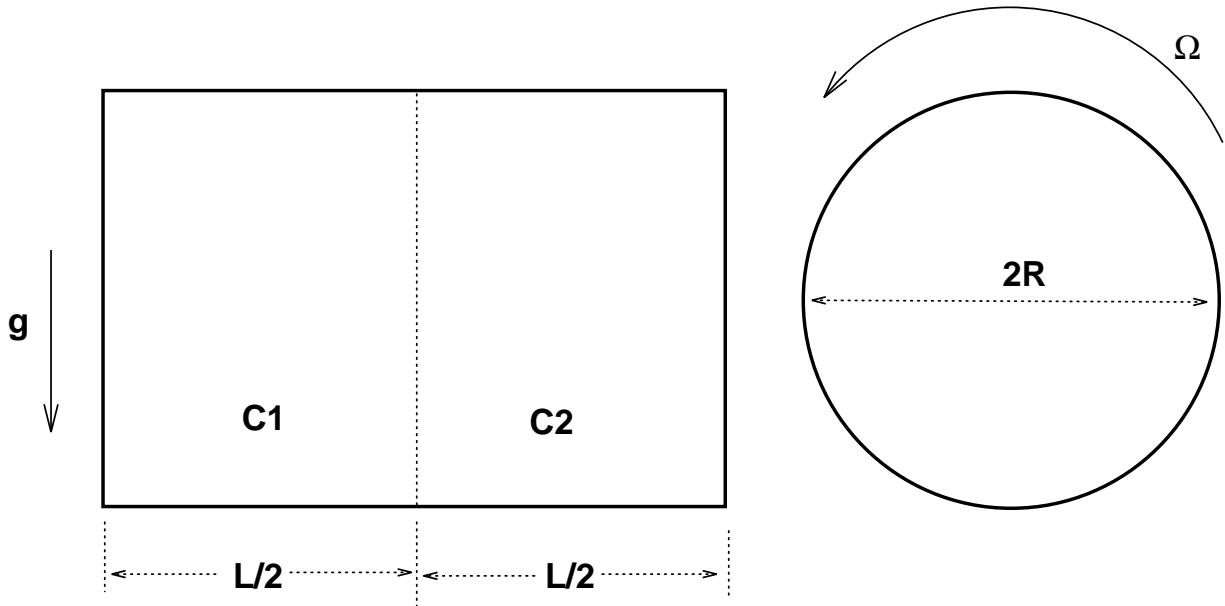


Figure 1: Schematic illustrating the experimental set-up. Initially the two material components, C1 and C2 are well separated.

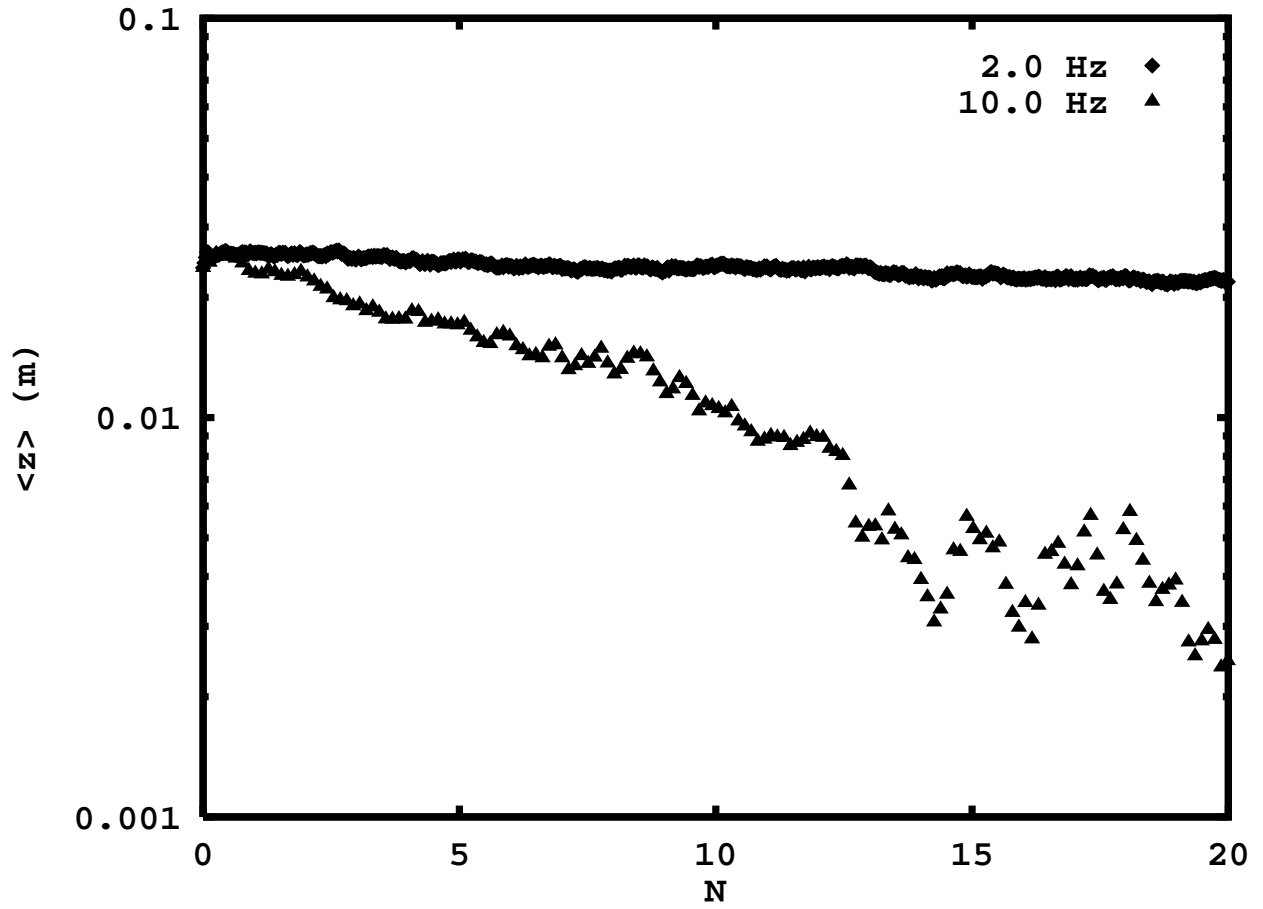


Figure 2: Self-diffusion: Average position as a function of the number of revolutions \mathcal{N} for two different rotation speeds.

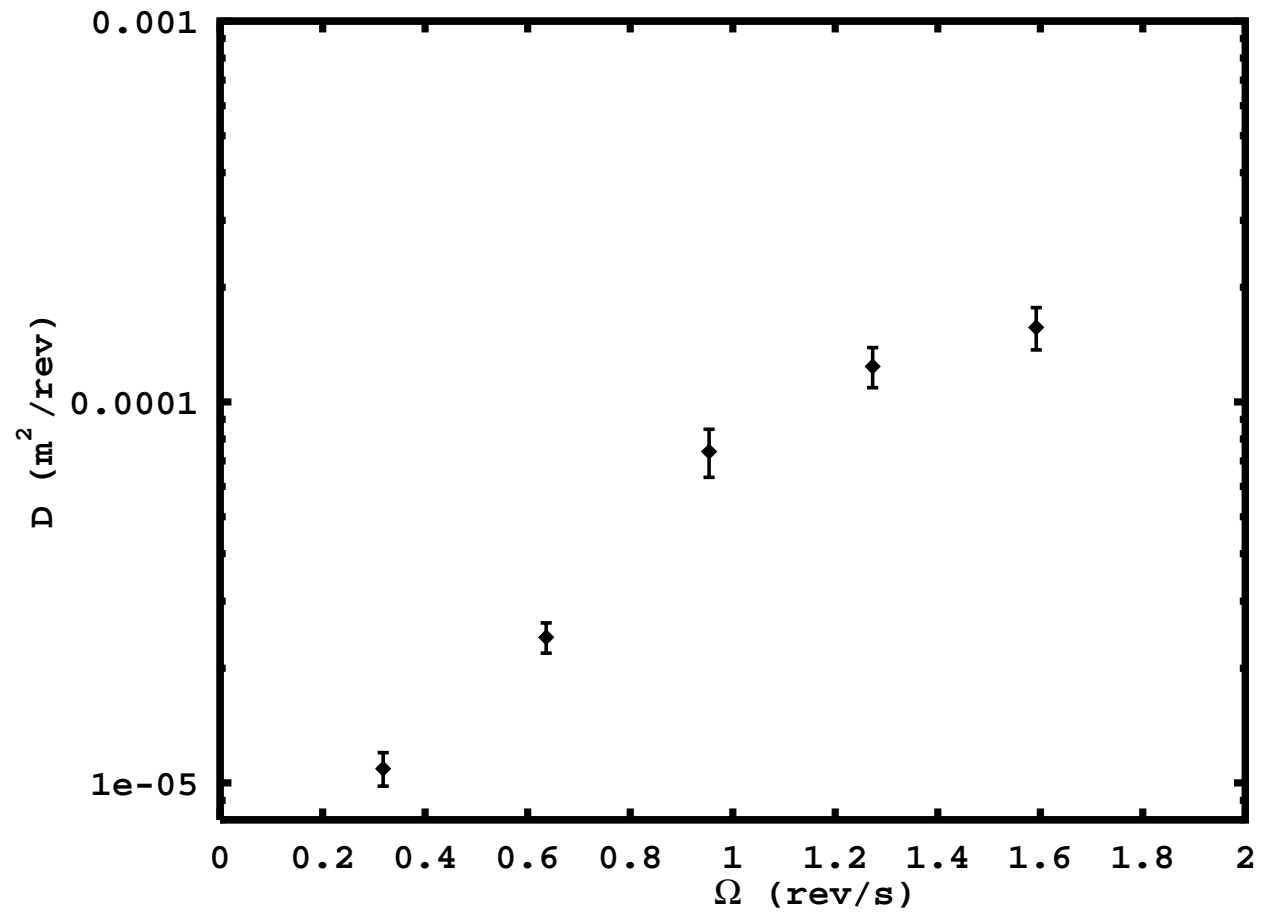


Figure 3: Diffusion coefficients for self-diffusion as a function of the number of revolutions.

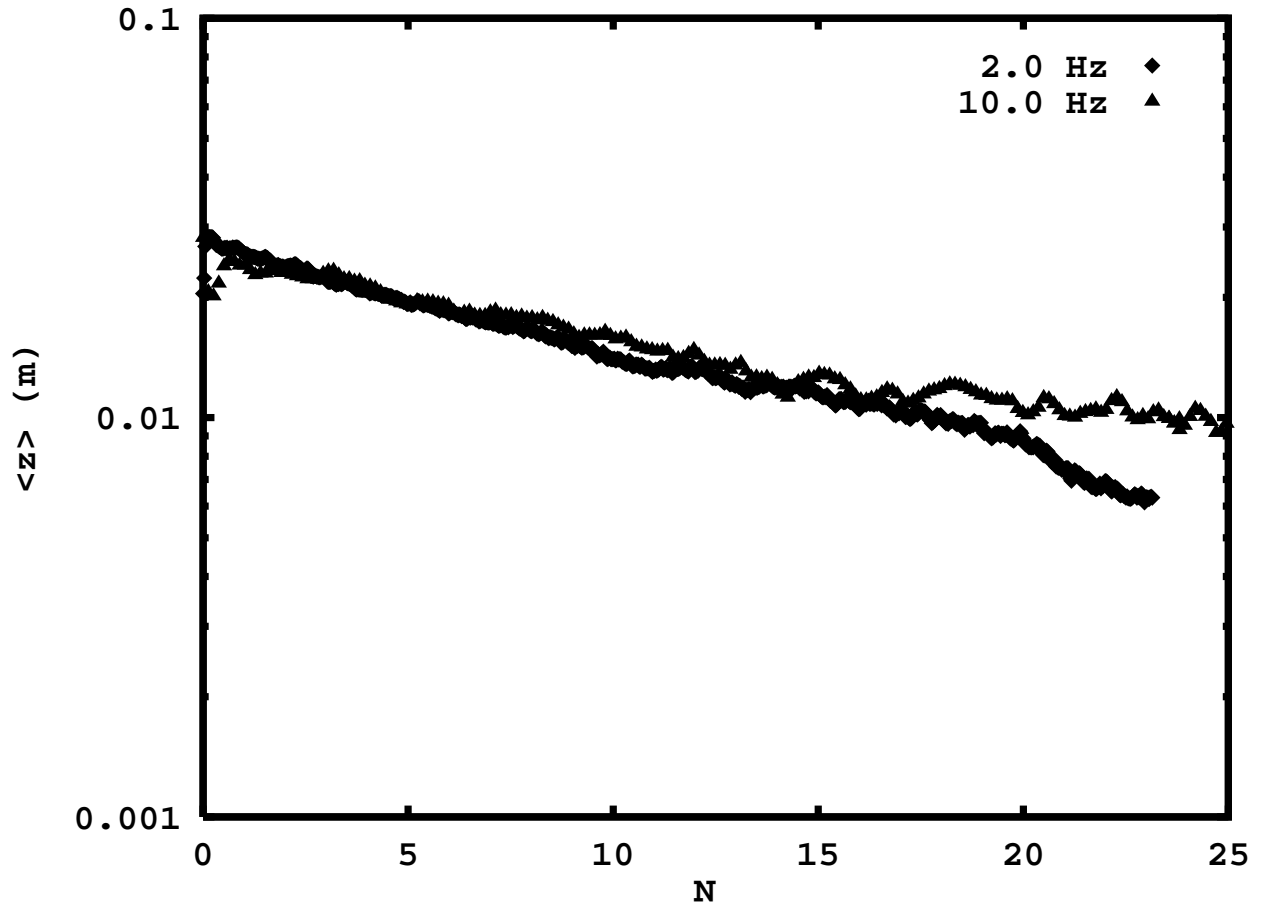


Figure 4: 2-Component diffusion: Average position as a function of the number of revolutions \mathcal{N} for two different rotation speeds.

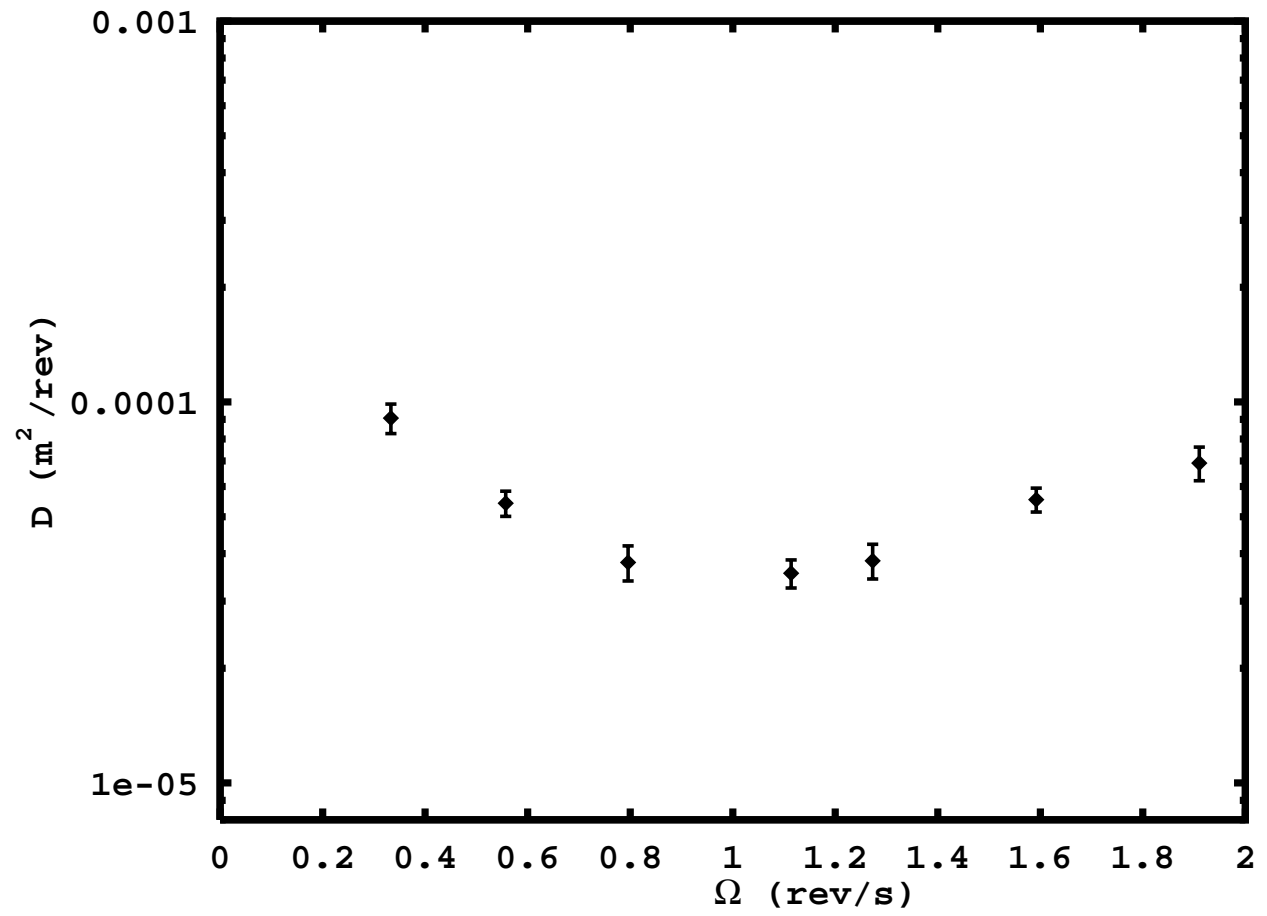


Figure 5: Diffusion coefficients for 2-component diffusion as a function of the number of revolutions.

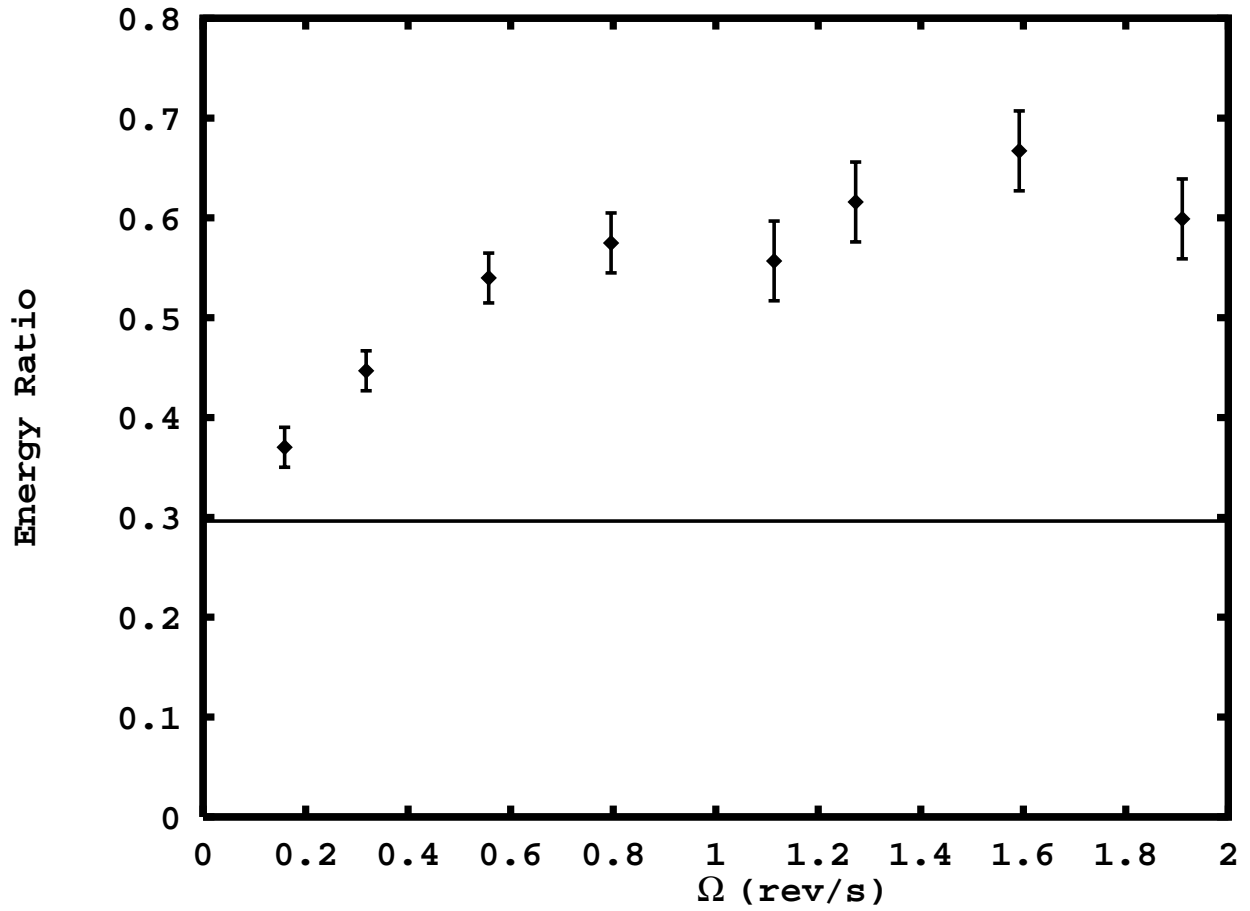


Figure 6: The ratio of the average kinetic energy for particles composed of material 2 to that for particles composed of material 1.